

Alma Mater Studiorum Università di Bologna
Archivio istituzionale della ricerca

Hybrid Silicon Nanocrystals for Color-Neutral and Transparent Luminescent Solar Concentrators

This is the final peer-reviewed author's accepted manuscript (postprint) of the following publication:

Published Version:

Mazzaro, R., Gradone, A., Angeloni, S., Morselli, G., Cozzi, P.G., Romano, F., et al. (2019). Hybrid Silicon Nanocrystals for Color-Neutral and Transparent Luminescent Solar Concentrators. ACS PHOTONICS, 6(9), 2303-2311 [10.1021/acsp Photonics.9b00802].

Availability:

This version is available at: <https://hdl.handle.net/11585/714769> since: 2024-05-28

Published:

DOI: <http://doi.org/10.1021/acsp Photonics.9b00802>

Terms of use:

Some rights reserved. The terms and conditions for the reuse of this version of the manuscript are specified in the publishing policy. For all terms of use and more information see the publisher's website.

This item was downloaded from IRIS Università di Bologna (<https://cris.unibo.it/>).
When citing, please refer to the published version.

(Article begins on next page)

This is the final peer-reviewed accepted manuscript of:

Hybrid Silicon Nanocrystals for self reabsorption-free and transparent Luminescent Solar Concentrators

R. Mazzaro, A. Gradone, S. Angeloni, G. Morselli, P. G. Cozzi, F. Romano, A. Vomiero, P. Ceroni

ACS Photonics **2019**, 6, 2303–2311

The final published version is available online at:
<https://doi.org/10.1021/acsp Photonics.9b00802>

Terms of use:

Some rights reserved. The terms and conditions for the reuse of this version of the manuscript are specified in the publishing policy. For all terms of use and more information see the publisher's website.

This item was downloaded from IRIS Università di Bologna (<https://cris.unibo.it/>)

When citing, please refer to the published version.

Hybrid Silicon Nanocrystals for self reabsorption-free and transparent Luminescent Solar Concentrators

Raffaello Mazzaro, Alessandro Gradone, Sara Angeloni, Giacomo Morselli, Pier Giorgio
Cozzi, Francesco Romano*, Alberto Vomiero, Paola Ceroni**

Dr. Mazzaro, R.,
CNR-IMM Bologna, Via Piero Gobetti 101. 40139, Bologna, Italy.
E-mail: mazzaro@bo.imm.cnr.it

Dr. Mazzaro, R., Prof. Vomiero, A.
Division of Materials Science, Department of Engineering Science and Mathematics, Luleå
University of Technology, 971 87 Luleå, Sweden.

Dr. Mazzaro, R.; Gradone, A.; Angeloni, S.; Morselli, G.; Prof. Cozzi, P.G.; Dr. Romano, F.;
Prof. Ceroni, P.
Chemistry Department “Giacomo Ciamician”, University of Bologna, 40129 Bologna, Italy.
E-mail: francesco.romano16@unibo.it; paola.ceroni@unibo.it

Prof. Vomiero, A.
Department of Molecular Sciences and Nanosystems, Ca’ Foscari University of Venice, Via
Torino 155, 30172 Venezia Mestre, Italy.

KEYWORDS Silicon Nanoparticles, Quantum dots, Photovoltaic devices, Organic dyes,
Anthracene, Energy transfer.

ABSTRACT One of the most detrimental loss mechanisms in Luminescent Solar Concentrators
(LSCs) is re-absorption of emitted light from the luminophore. Silicon Nanocrystals (SiNCs) offer

This item was downloaded from IRIS Università di Bologna (<https://cris.unibo.it/>)

When citing, please refer to the published version.

a solution due to the high apparent Stokes-shift, but the poor absorption properties limit their performance as LSCs luminophore. Coupling an organic dye to SiNCs represents a smart approach to obtain sensitization of SiNCs luminescence by the organic dyes, thus resulting in tunable and improved optical properties of LSCs. In particular, 9,10-diphenylanthracene was employed as UV sensitizer for SiNCs in order to produce LSCs with aesthetic appearance suitable to smart window application and optical efficiency as high as 4.25%. In addition, the role of the energy transfer process on LSC performance was elucidated by a thorough optical and photovoltaic characterization.

Luminescent Solar Concentrators (LSCs) were proposed for the first time in 1973¹ as a viable alternative route to traditional Si-based solar panels, aiming at reducing the electricity costs and offering a solution suitable for Building Integrated Photovoltaics (BIPV). After a period of silence, mainly driven by the low cost of oil in the eighties, the research re-discovered this architecture in the latest years, thanks to the development of engineered luminophores, guaranteeing improved optical properties compared to standard organic dyes².

LSC architecture consists in a plastic plate embedded with luminescent species that extensively absorb sunlight and emit in a spectral window where conventional Si-cells or GaAs cells have high power conversion efficiency. A substantial portion of the light emitted by the luminescent species can be concentrated to the edge of the plate (up to ~75% according to Snell's law² for a polyacrylate waveguide) by total internal reflection. The advantages provided by this simple setup are related mostly to the possibility of preparing large area polymer plates with relatively simple procedures and low cost, coupling it to small area, band-gap matched and highly efficient

This item was downloaded from IRIS Università di Bologna (<https://cris.unibo.it/>)

When citing, please refer to the published version.

conventional PV cell. Advanced solutions include also sandwich structures, in which front and bottom glass panels can improve light transport, by decreasing light reflection at the plastic surface and re-absorption losses inside the active medium³. In addition, this architecture allows the preparation of transparent and colored polymer plates that can be used as large panels in windows and facades, following the BIPV approach^{4,5}.

The record power conversion efficiency for an LSC-coupled PV cell is about 7.1% and it is reported for a luminescent organic dye based LSC⁶. However, this value is not informative since it is highly dependent on the dimension of the LSC and on the amount of light absorbed by the LSC: colorless LSC absorbing only the UV component of the solar spectrum has a lower efficiency⁷, but are best suited as smart windows. Several other classes of luminophores have been employed in LSC devices, such as metal nanoclusters⁸, lanthanides hybrids⁹, conjugated polymers¹⁰ and molecular aggregates¹¹, but these approaches have been followed by limited development due to either limited performance or poor stability.

In the last few years, the interest has moved towards LSC based on nanorods and quantum dots¹². These luminophores appear as fascinating materials thanks to their optical properties, namely higher photostability and simpler tunability of the luminescence color. Several examples are reported embedding Cd^{13–16}, Pb^{17,18} and perovskite-based^{19–21} quantum dots, obtaining relatively good efficiencies. Recently some concerns about the use of toxic heavy metals in these applications are emerging. As a consequence, research is now focused on heavy metal free QDs such as CuInS_xSe_{2-x} and Mn²⁺-doped ZnSe QDs^{22,23}, carbon dots^{24,25} and silicon nanocrystals (SiNCs).

SiNCs represent an interesting alternative to conventional binary or ternary alloy-based QDs for multiple reasons²⁶: (i) viability and abundance of the main component, (ii) lack of toxicity, (iii) robust surface functionalization by covalent bond, which ensures stability and dispersibility in

This item was downloaded from IRIS Università di Bologna (<https://cris.unibo.it/>)

When citing, please refer to the published version.

different polymer matrices, (iv) tunable and size-dependent photoluminescence properties²⁷ and (v) apparent large Stokes-shift related to their indirect band-gap nature. The last feature results in negligible reabsorption in bulk polymer LSCs based on SiNCs, producing competitive optical efficiency with a non-toxic, widely available luminescent material, as described in a seminal paper by Meinardi et al.²⁸. Despite the extremely promising results, the peculiar optical properties of SiNCs come with some downsides, mainly arising from the poor absorption properties. Indeed, due to the indirect nature of the optical transition, the absorption coefficient is scarce in the visible region and gradually increases in the UV region, in contrast to the abrupt transition usually observed in direct band gap QDs. Thus, in order to efficiently harvest the solar spectrum, a large concentration of SiNCs must be employed.

An accurate control on the shape of the absorption features is of the utmost importance for the preparation of LSCs absorbing mainly in the UV-A region of the solar spectrum ($\lambda = 350\text{-}400\text{ nm}$), to be employed in BIPV. For conventional QDs, this is usually achieved by inorganic core-shell structures or doping the material with transition metals²⁹, where a high band-gap semiconductor is responsible for the light absorption in the UV region and luminescence derives from the lower band-gap semiconducting material. This approach has not been applied to SiNCs yet, since the luminescence is strongly sensitive to surface chemistry, typically producing partial or complete quenching of the nanocrystal, instead of luminescence tuning.

An appealing alternative approach employs an organic-inorganic hybrid material: organic chromophores covalently attached to the surface of SiNCs absorb light and funnel the excitation energy to the silicon core, the working principle of a light-harvesting antenna³⁰. As already proved by our group, this approach is feasible with an efficient sensitization of the luminescence of colloidal SiNC upon excitation in the UV^{31,32}, visible³³ and also NIR³⁴ spectral region. By this

This item was downloaded from IRIS Università di Bologna (<https://cris.unibo.it/>)

When citing, please refer to the published version.

approach it is possible to tune the absorption properties of the material and to preserve the luminescence properties of the silicon core.

This work reports the synthesis and characterization of colloidal silicon nanocrystals functionalized with 9,10-diphenylanthracene (DPA) derivatives and the preparation of polymer LSCs based either on this new hybrid luminophores or on a physical mixture of DPA and SiNCs. The DPA chromophore was selected because it absorbs in the UV-A spectral region and it does not affect the optical appearance in the visible region. Energy transfer from DPA to SiNCs is expected to occur for both LSCs via non-radiative or radiative mechanism. Thorough optical and photovoltaic characterization is performed to investigate the properties of the prepared LSC devices and to elucidate the role of the energy transfer process on them.

RESULTS AND DISCUSSION

SiNCs were produced by thermal disproportionation of hydrogen silsequioxane (HSQ, $[\text{HSiO}_{3/2}]_n$) to obtain Si nanocrystals embedded in SiO_2 . Etching the oxide matrix with HF yields free-standing H-terminated Si nanocrystals^{35–37}. The surface functionalization of hydride-terminated SiNCs consisted in a two-step procedure: (i) hydrosilylation with chlorodimethylvinylsilane promoted by diazonium salts (4-decylbenzene diazonium tetrafluoroborate),³⁸ yielding chlorosilane-passivated SiNCs (**Figure 1a**), (ii) post-functionalization by nucleophilic reagents: in the present case, the acetylide derivative of diphenylanthracene formed in situ with nBuLi, yielding the **Si-DPA** sample.

As control sample, alkyl-capped SiNCs (**Si**) were prepared by hydrosilylation of hydrogen-capped silicon nanocrystals in presence of 1-dodecene and initiated with diazonium salt (**Figure 1b**).

This item was downloaded from IRIS Università di Bologna (<https://cris.unibo.it/>)

When citing, please refer to the published version.

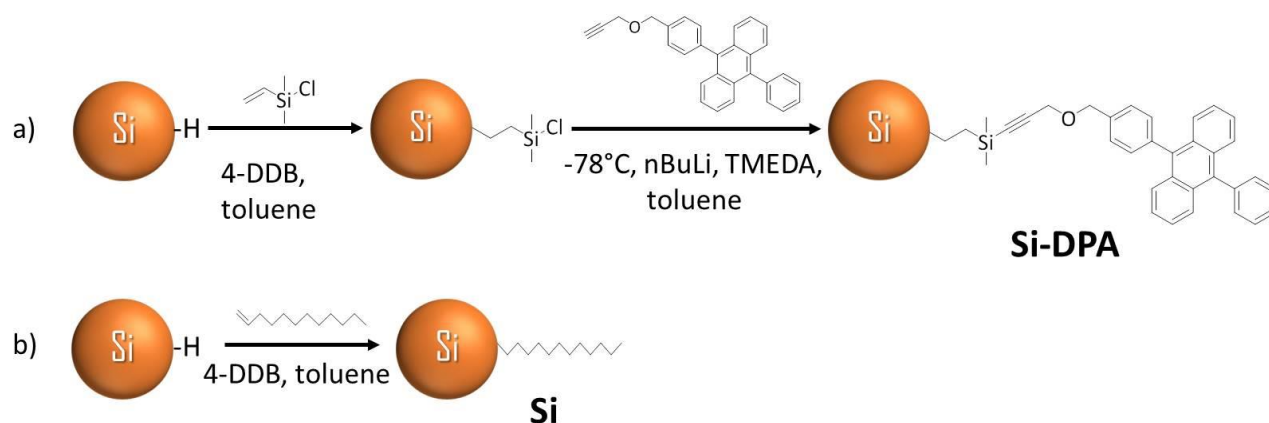


Figure 1. Schematic representation of the synthesis of (a) SiNCs covalently functionalized with 9,10-diphenylanthracene chromophores (**Si-DPA**) and (b) alkyl-passivated SiNCs sample (**Si**).

Photophysical characterization in solution

The absorption and photoluminescence (PL) spectra of **Si-DPA** samples in toluene solution are reported in **Figure 2** (green line). The absorption spectrum exhibits the typical featureless absorption of the silicon core gradually increasing in the UV region, as observed for **Si** sample, plus the structured and sharp band of the diphenylanthracene chromophore limited to the UV-A region. The overall spectrum perfectly matches the one of the control sample constituted by a physical mixture of **Si** and **DPA** (**Si+DPA**, red line) with the same concentration, suggesting that no ground state interaction is affecting their optical properties. On the basis of the molar absorption coefficients of DPA ($\epsilon_{375\text{nm}} = 1.4 \times 10^4 \text{ M}^{-1} \text{ cm}^{-1}$) and SiNCs ($\epsilon_{430\text{nm}} = 1 \times 10^5 \text{ M}^{-1} \text{ cm}^{-1}$ for 3.5 nm diameter, see SI for more details), we can estimate an average number of ca. 80 DPA fluorophores per SiNC, resulting in a strong enhancement of the absorption properties of the **Si-DPA** upon excitation in the $\lambda = 350\text{-}400 \text{ nm}$ region.

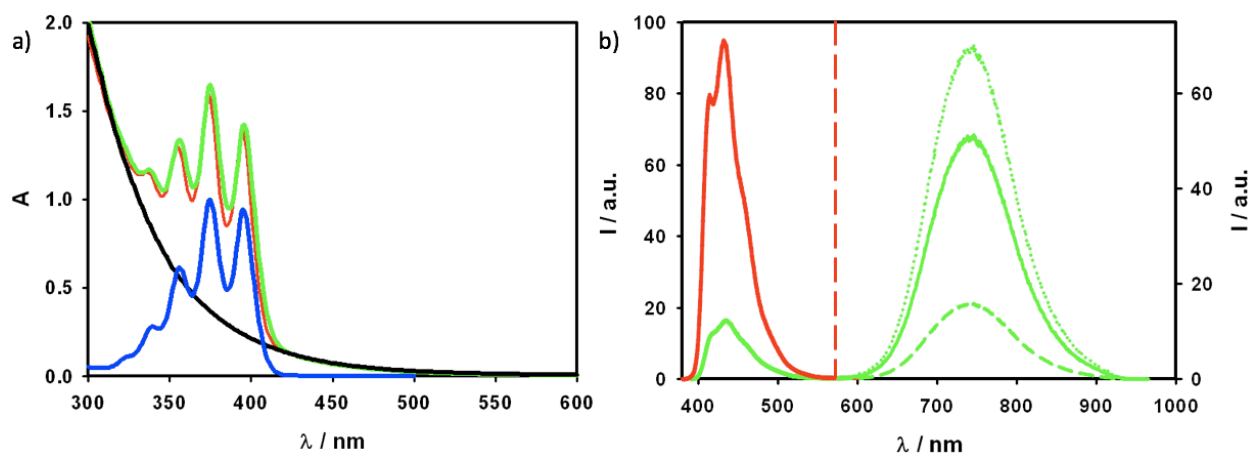


Figure 2. a) Absorption spectra of **Si** (black line), **Si-DPA** (green line), **DPA** (blue line), and a physical mixture of **Si** and **DPA** (**Si+DPA**, red line) with the same concentration as that of the covalent sample. b) PL spectra of **Si-DPA** (green solid line, $\lambda_{\text{ex}} = 375$ nm) and **Si+DPA** (red line, only DPA contribution, $\lambda_{\text{em}} = 390\text{-}580$ nm) of two isoabsorbing solutions at the excitation wavelength of 375 nm. For the sake of comparison, the PL spectra of **Si-DPA** corresponding to 100% energy transfer (dotted green line) and 0% energy transfer (dashed green line) are reported (for more details, see SI). All spectra are registered at room temperature in air-equilibrated toluene.

Upon excitation at 375 nm, where most of the light (80%) is absorbed by **DPA** chromophores in the **Si-DPA** sample, two emission bands are observed (green line in **Figure 2b**): one structured-band centered at 440 nm and the other at ca. 750 nm. The high energy band is assigned to the diphenylanthracene fluorescence and the low energy band is due to the Si core emission, by comparison with the PL spectra of **DPA** and **Si**. Indeed, the band centered at 440 nm is observed also in the control sample **Si+DPA**, the lower intensity of DPA band in the covalent sample being due to a quenching process. The quenching efficiency (η_q) is estimated to be 82% (see SI for additional details) and it is due to a photoinduced energy transfer from diphenylanthracene to the

Si core, as demonstrated by the sensitization of the Si core emission at 750 nm. Indeed, a close match of the excitation spectrum performed at the SiNC emission ($\lambda_{em}=750$ nm) and the absorption spectrum of **Si-DPA** is observed (**Figure S3**). The sensitization efficiency (η_s) is estimated to be 70% (see SI for additional details), pointing to a very efficient energy transfer.

The PL quantum yield (PLQY) of the SiNCs in the **Si-DPA** sample is measured upon selective excitation of the Si core at 460 nm: the resulting value is 26%, lower than that observed for the **Si** sample (45%) under the same experimental conditions. Accordingly, the PL decay time is shorter (50 μ s) in **Si-DPA** compared to **Si** (90 μ s). The same effect has been previously reported by some of us in the case of SiNCs functionalized by different organic chromophores^{31,33,34}; it is likely due to the presence of more defects at the surface of the **Si-DPA** sample, compared to the **Si** sample. In this case, it is worth noting that the control sample (**Si**) has been obtained by a different synthetic procedure (**Figure 1**) and this may impact on the resulting PLQY.

LSC preparation and optical properties

LSCs were obtained by thermal polymerization of an MMA/LMA monomer blend, in presence of the luminophores and EGDM as cross-linking agent. LSCs based on different combinations of chromophores were prepared: (i) alkyl-capped SiNCs (**Si**), (ii) pure DPA chromophores (**DPA**), (iii) SiNCs covalently functionalized with DPA units (**Si-DPA**), (iv) a physical mixture of SiNCs and DPA (**Si+DPA**) with the same absorbance as the covalent sample, in order to investigate the role of the covalent bond with respect to the LSC optical performance.

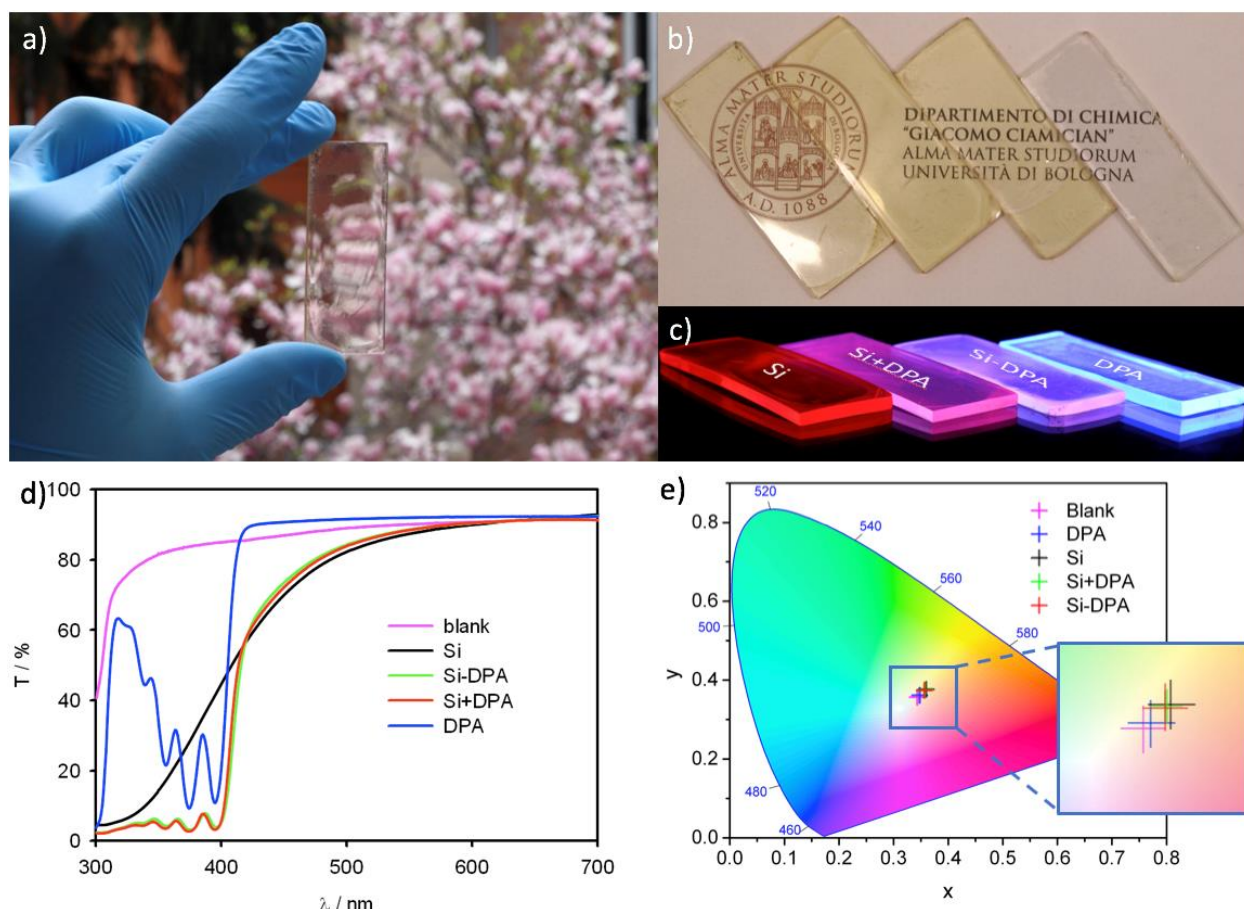


Figure 3. Digital picture of the SiNCs based LSCs under visible (a, b) and UV illumination (c). UV-Vis transmittance spectra of the same LSCs (d) and CIE 1931 color space chromaticity diagram reporting the color coordinates of the SiNCs based LSCs (e).

The prepared LSCs are transparent and almost colorless (**Figure 3a and b**), but they display distinctive PL colors upon UV illumination (**Figure 3c**). By comparing the absorption spectra in the low energy region ($\lambda_{abs} = 600\text{-}700\text{ nm}$), no evidence of aggregation is observed and the average transmittance is higher than 85% (**Figure 3d**), proving the excellent degree of transparency of the prepared polymer slabs and the lack of scattering centers. As previously

This item was downloaded from IRIS Università di Bologna (<https://cris.unibo.it/>)

When citing, please refer to the published version.

observed in solution phase, both the featureless absorption band of SiNCs and the structured DPA band are visible. The fraction of photons absorbed in the visible region of the solar spectrum $\eta_{\text{abs-vis}}$ ($\lambda_{\text{abs}} = 400\text{-}700$ nm, integrated from transmittance spectra on AM 1.5G spectrum, **Table 1**) ranges from 13% of the blank sample, whose apparently high value is due to surface roughness and incident light trapping in the waveguide, to 27% of the **Si** sample. Since the absorptance is providing only limited information about the visual appearance of the semi-transparent slab, we calculated the color coordinates and the Color Rendering Index (CRI) using the CIE 1931 chromaticity diagram (details reported on the experimental section).

Table 1. Absorption properties (fraction of absorbed photons in the visible range, $\lambda_{\text{abs}} = 400\text{-}700$ nm) and color coordinates of the prepared LSCs.

	$\eta_{\text{abs-vis}}$	x	y	CRI
blank	13%	0.344	0.356	99.0
DPA	14%	0.348	0.361	98.4
Si	27%	0.360	0.376	97.0
Si+DPA	24%	0.358	0.375	96.8
Si-DPA	24%	0.357	0.374	97.0

The color coordinates of the LSCs (**Table 1**) are located in the central region of the chromaticity diagram reported in **Figure 3e**, indicating good achromatic or neutral color sensations with only a small shift towards the yellow-orange region. The CRI values range from 99.0% for the blank sample to 96.8% for **Si+DPA** sample. No shift is observed upon addition of DPA, proving that the organic chromophore is only contributing to the absorption of the UV portion of the solar

This item was downloaded from IRIS Università di Bologna (<https://cris.unibo.it/>)

When citing, please refer to the published version.

spectrum. These values lie in the color rendering group 1, fulfilling the highest CIE requirements for indoor and outdoor illumination.

We then compared the PL properties of LSCs (**Figure 4**): in all samples the DPA band at 430 nm is significantly red-shifted with respect to the PL spectrum registered in solution (**Figure 2b**) and PLQY drops from 95% for DPA in solution³⁹ to 57% for **DPA** sample in the polymer matrix. Re-absorption of emitted light is responsible for both the red-shift and the decrease of PLQY: re-absorption processes are amplified in the LSC architecture by the long optical path in the polymeric waveguide compared to solution phase. A further drop of DPA fluorescence is observed in **Si-DPA** and **Si+DPA** samples. The strong drop in PL intensity in the **Si-DPA** sample was previously observed in solution and results from the non-radiative energy transfer process. On the contrary, the quenching of DPA PL in **Si+DPA** sample is related to a trivial energy transfer process. Indeed, due to the amplified re-absorption processes in the long optical path LSCs, there is much larger probability for the light emitted by DPA to be re-absorbed by SiNCs. The mechanisms of the quenching processes is further confirmed by the analysis of the decay of DPA fluorescence intensity (**Figure S4**): a shorter decay, corresponding to a lifetime of 2.5 ns, is observed for **Si-DPA**, compatible with the presence of a new non-radiative process for the deactivation of the fluorescent excited state of DPA, while **Si+DPA** sample exhibits similar lifetime with respect to pristine **DPA**, about 8.5 ns and 7.2 ns, respectively.

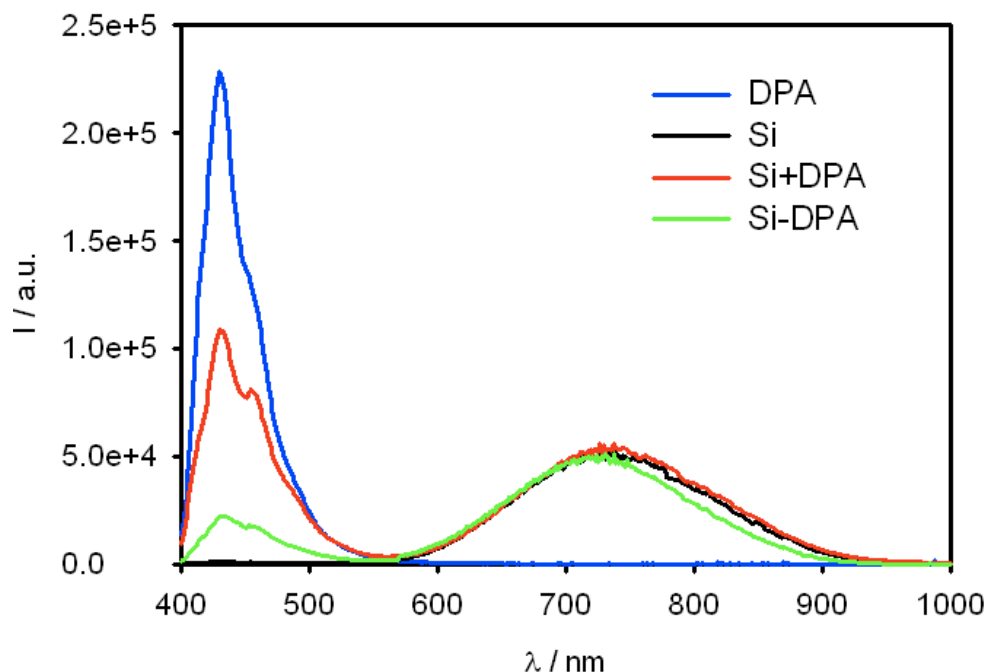


Figure 4. PL spectra of **Si** (black line), **DPA** (blue line), **Si+DPA** (red line) and **Si-DPA** (green line) measured inside an integrating sphere by excitation of the larger surface of LSCs at 375 nm. For the sake of comparison, the low energy band at 750 nm of **Si-DPA** was normalized on the PLQY of sample **Si**.

The SiNCs PL band at 750 nm is not significantly affected by embedding in the polymer matrix in terms of both shape and intensity: upon selective excitation of the Si core at 450 nm, PLQY is 43%, 45% and 27% for **Si**, **Si+DPA** and **Si-DPA**, respectively, values comparable to those measured in solution phase (45% for **Si** and **Si+DPA**, 26% for **Si-DPA**). Upon excitation at 375 nm, no difference in the emission intensity at 750 nm is observed for **Si**, **Si+DPA** and **Si-DPA** (after normalization for the intrinsic PLQY drop for SiNCs, **Figure 4**).

SiNCs PL intensity (upon excitation at 375 nm) is expected to be affected by two opposite effects: (i) the inner filter effect decreases the SiNCs luminescence intensity, i.e. SiNCs absorbs a reduced

amount of light in **Si+DPA** and **Si-DPA** samples with respect to **Si** sample because of the co-absorption of DPA chromophores; (ii) the energy transfer process occurring for **Si+DPA** and **Si-DPA** samples increases the SiNCs luminescence intensity. The lack of observable PL intensity changes in **Si+DPA** and **Si-DPA** samples compared to the pristine **Si** sample proves that the two effects are counterbalanced. Consistently, by applying a mathematical correction for the inner filter effect to the registered spectra (**Figure S5**), both **Si+DPA** and **Si-DPA** samples exhibit higher PL intensity with respect to **Si** sample. This proves the sensitization of SiNCs PL by DPA in both samples with similar efficiency, despite the different energy transfer mechanism described in the previous section.

In order to get information about the optical efficiency of the LSC, we estimated the ratio of photons emitted from the edges of the LSC with respect to the ones emitted by the whole LSC device $\left(\frac{I_{edges}}{I_{tot}}\right)$, as previously reported by Coropceanu et al.⁴⁰. Upon excitation at 450 nm, where only the silicon core absorbs light, the ratio is about 74% for all samples containing SiNCs, a value close to the maximum theoretical efficiency of 75% predicted by Snell's law for a polyacrylate waveguide ($\eta_{TR} = \sqrt{1 - \frac{1}{n^2}} = 75\%$): this is a demonstration of i) the scattering-free propagation of the emitted light in the polymer matrix due to the good affinity between the hybrid dyes and the polymer host, ii) lack of re-absorption, allowing an extremely high light trapping efficiency. Upon excitation at 375 nm, where the absorption contribution of DPA is at its maximum, **Si** has similar values to the one reported by exciting at 450 nm, while $\left(\frac{I_{edges}}{I_{tot}}\right)$ values decrease to 56% and 54% for **Si+DPA** and **Si-DPA** samples, respectively. This drop is related to re-absorption losses of DPA

PL, much stronger than that of the Si core PL. Indeed, **DPA** sample shows a much lower value of this ratio ($\frac{I_{edges}}{I_{tot}} = 31\%$). Indeed, being the emission by randomly oriented DPA chromophores isotropic, the occurrence of multiple re-absorption and PL processes induces a randomization of the optical path followed by the emitted photons, and a consequent increased probability of photon losses from the top of the waveguide through the escape cone⁴¹.

Further indication of this phenomenon can be assessed by comparing the PL spectra obtained from the edge of the LSC at increasing excitation distance (**Figure 5**).

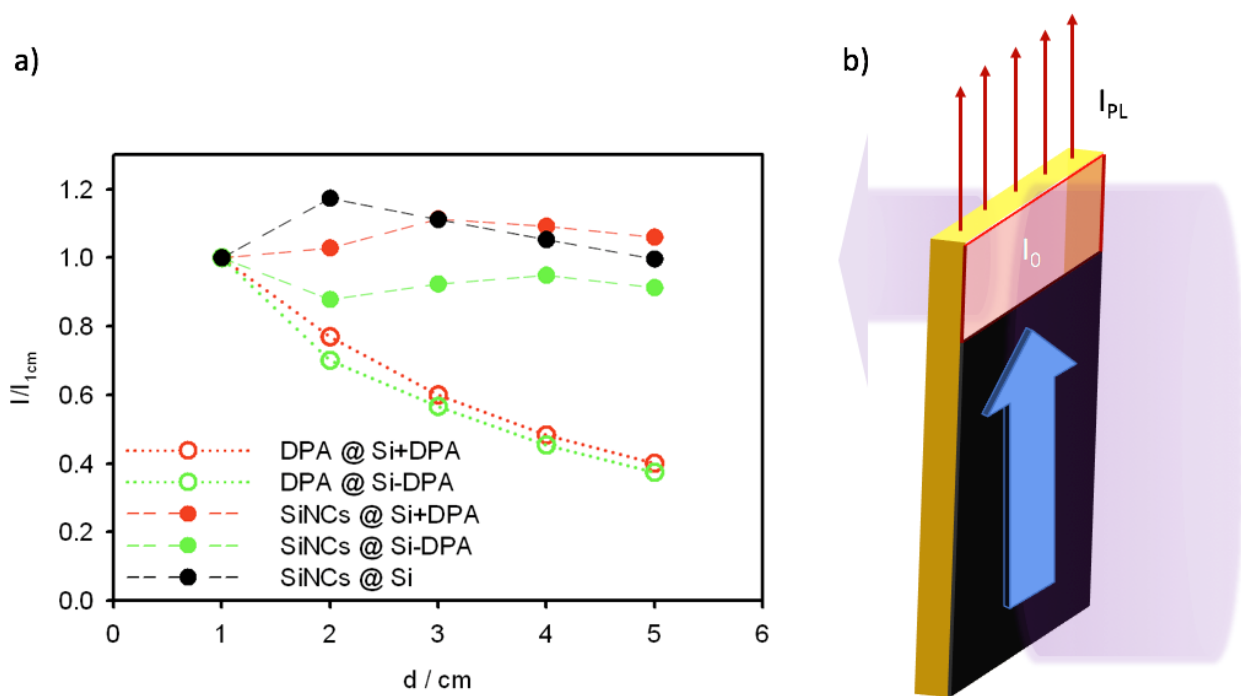


Figure 5. a) Normalized emission intensities of diphenylanthracene ($\lambda_{em} = 400-550$ nm, open symbols) and SiNC ($\lambda_{em} = 550-900$ nm, solid symbols) of **Si+DPA** (red), **Si-DPA** (green) and **Si** (black) as a function of the distance between the excitation area on the top of the polymer slab and the emission registered on one of the edges of the slab, as depicted in the schematic representation

reported in panel b). The intensity was normalized to the illuminated area and to the emission intensity obtained at 1 cm from the excitation.

The shape of the SiNC emission band at 750 nm is not affected by the distance between the excitation spot on the top of the polymer slab and the emission registered on one edge of the slab in **Si-DPA** (**Figure S7a**), **Si+DPA** (**Figure S7b**) and **Si** (**Figure S7c**), whereas the DPA fluorescence band at 430 nm is strongly red-shifted upon increasing the distance between excitation and emission because of the above-discussed re-absorption phenomena. As far as intensity is concerned, the SiNCs PL band intensity is almost stable upon increasing the distance between excitation and detection (**Figure 5**, solid symbols), while DPA PL intensity is dropping as a function of distance (**Figure 5**, open symbols). By fitting this decreasing trend with an exponential curve, the expected intensity value of DPA fluorescence after 20 cm of optical path is about 14% of the starting PL value extrapolated at 0 cm. The ratio between DPA and SiNCs PL intensity as a function of the distance between excitation and emission shows the sole contribution of SiNCs at large distances for both **Si+DPA** and **Si-DPA** samples (**Figure S8d**). A larger contribution of DPA PL in the low distance-regime is visible for **Si+DPA**, while **Si-DPA** sample is characterized by less variability across the distance range, since most of DPAs quenching process is non-radiative and does not depend on the optical path.

The photostability of the LSCs was evaluated by irradiating the samples for 48h with AM 1.5G simulated light. The measured spectra for **Si-DPA** and **Si+DPA** samples are reported in figure S8 and display a relatively slow degradation both for DPA and SiNCs PL contributions. A large drop of PL intensity is observed for SiNCs in both samples in the first 8h, after which the PL intensity stabilizes. On the opposite, the PL intensity of DPA follows a quasi-linear trend. While the overall

This item was downloaded from IRIS Università di Bologna (<https://cris.unibo.it/>)

When citing, please refer to the published version.

intensity drop is higher for SiNCs due to the initial degradation, SiNCs are more stable in the long term. Indeed, for **Si+DPA** sample, the DPA intensity after 48h is about 75% of the one measured after 8h, while the one of SiNCs is about 86%. Similarly, the ratios observed for **Si-DPA** sample are 79% and 89% for DPA and SiNCs PL contributions, respectively.

Photovoltaic performance

The photovoltaic performance of our LSCs was evaluated by placing a custom-sized Si-PV cell on one edge of the slab and letting the residual edges uncovered. Irradiation was perpendicular to the slab surface with a conventional AM 1.5G solar simulator. We carried out a scan of the JV characteristic, from which we calculated the main PV parameters for the different samples, reported in **Table 2**. The shape factor, called G factor and defined as the ratio between the surface of the top of the slab and the edges surface, was calculated considering the surface of all edges as active (**Table S1**).

Table 2. Main PV parameters extracted from JV characteristics of a Si-PV cell attached to one side of the prepared LSCs. G-factor and η_{opt} are also reported, as described in the main text.

	G	Jsc / mA/cm²	Voc / mV	FF / %	PCE / %	η_{opt} / %	<math>\eta_{\text{opt, abs- vis}}</math> %
Blank	2.86	1.31	382	54	0.27	1.04	-
DPA	2.70	4.05	463	62	1.16	3.59	_*
Si	2.64	4.14	452	60	1.12	3.54	25.7

Si+DPA	2.56	4.79	455	61	1.33	4.25	38.8
Si-DPA	2.98	4.05	440	59	1.05	3.08	28.1

* DPA $\eta_{\text{opt, abs-vis}}$ was not calculated due to negligible absorption contribution in the visible region of the solar spectrum.

The area of the concentrator, physically in contact with the cell surface, was considered for the estimation of the short-circuit current density (J_{SC}). A comparison of the blank sample with the other samples evidences a slight increase in the open circuit voltage (V_{OC}) and the Fill Factor (FF) and a strong increase in J_{SC} , directly proportional to the increased emitted photon flux incident on the PV cell, resulting in a large enhancement of PCE values. The J_{SC} for the blank sample is not negligible due to the trapping of the incident light in the polymer waveguide, whose contribution, whereas minimal, cannot be fully avoided. As a consequence, this value can be considered as a baseline for the evaluation of the optical efficiency of the other LSCs.

DPA and **Si** samples display very similar results in terms of PCE, since the higher PLQY of **DPA** is counterbalanced by the lack of re-absorption of **Si**, achieving similar results on this size scale. We expect much larger values for **Si** compared to **DPA** upon scaling-up the devices to larger size.

The **Si+DPA** sample is characterized by a PCE enhancement of about 15-20% with respect to the pristine **DPA** and **Si** sample. On the opposite, the PCE of **Si-DPA** is slightly decreased because of the lower PLQY of the silicon nanocrystals, as discussed in the solution phase characterization.

More information about the concentration efficiency of the LSC can be extracted from the optical efficiency (η_{opt}) defined as follows⁴²:

This item was downloaded from IRIS Università di Bologna (<https://cris.unibo.it/>)

When citing, please refer to the published version.

$$\eta_{opt} = \frac{J_{LSC}}{J_{SC} \times G}$$

where J_{LSC} is the current density of the PV cell coupled to the LSC (i.e., J_{SC} values reported in **Table 2**), J_{SC} is the current density of the same cell under direct illumination, i.e. 44 mA/cm² in our setup, and G is the previously described size factor. The trend is exactly the same of that observed for PCE values with a minimum 3-fold enhancement factor with respect to blank sample. For comparison purpose, a previous paper on SiNCs based LSC reports²⁸ an $\eta_{opt} = 2.85\%$, slightly lower than the one reported hereby for the reference **Si** sample, but in the same efficiency range. Again, **Si+DPA** sample exhibits a robust increase with respect to pristine **Si**, proving that the physical mixture of SiNCs and DPA allows for an enhancement of the LSC performance. This suggests that the **Si+DPA** non-covalent approach is an effective strategy to enhance SiNCs performance in LSCs. The same trend is observed also applying the re-shaping factor, as previously suggested¹⁴, in order to take into account the mismatch between PV cell EQE and PL spectra of the luminophores (**Table S1**). The largest increase in $\eta_{opt,q}$ is displayed by the DPA sample due to the poor match between c-Si EQE spectrum and PL band in the high-energy region of the Visible spectrum, while smaller enhancement is observed for all samples containing SiNCs. This proves the superior spectral superposition between SiNCs-based LSCs and the most employed conventional c-Si PV cells.

On the other hand, while the covalent approach employed in **Si-DPA** does not positively influence optical efficiency and PCE, the absolute value has to be evaluated as a function of the absorption properties and the PLQY of the luminophore. **Table 1** reports the fraction of photons absorbed in the visible region ($\eta_{abs-vis}$) by the different LSCs. We estimated the corrected optical efficiency $\eta_{opt,abs}$ by dividing η_{opt} by $\eta_{abs-vis}$. This value is different from the internal optical

This item was downloaded from IRIS Università di Bologna (<https://cris.unibo.it/>)

When citing, please refer to the published version.

efficiency reported elsewhere, since it does only take into account the absorption contribution in the visible region. Therefore, its purpose is to compare performances of LSCs with different absorptances in the visible region, where the aesthetical and functional properties of the LSC are defined. Both **Si-DPA** and **Si+DPA** samples exhibit higher optical efficiency than **Si**, proving the enhancement related to SiNCs sensitization from the organic DPA chromophores. Interestingly, an enhancement was observed also for the **Si-DPA** sample, despite the lower PLQY resulting from the functionalization process, pointing out that the sensitization resulting from DPA absorbing in the UV region is able to compensate the detrimental drop of PLQY resulting from the synthetic procedure, in case of perfectly iso-absorbing SiNCs in the visible region.

Finally, a comparison between the photovoltaic response of the prepared LSCs as a function of the distance between the PV cell and the excitation position was performed, by analogy with the optical characterization previously discussed (**Figure 6**).

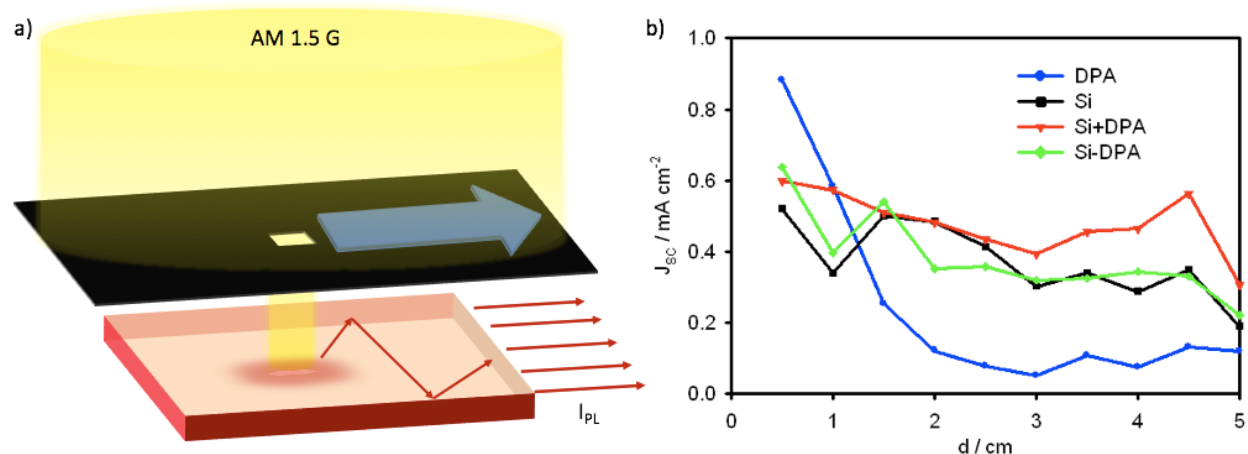


Figure 6. a) Schematic representation of PV response of the prepared LSCs as a function of the distance between the excitation spot on the top of the polymer slab, and the PV cell, located on one edge of the slab. b) Short circuit current densities, upon excitation of a $0.5 \times 0.5 \text{ cm}^2$ area, as a function of the distance between the center of the excitation area and PV cell. The contribution of

direct excitation was removed by subtracting the reference values obtained with a blank polymer slab.

The short circuit current density values measured for the samples containing SiNCs are basically constant across the LSC main axis, consistent with the behavior discussed within the optical characterization and typical for LSCs based on re-absorption free luminophores. The absolute values are close, but a slight enhancement can be observed for the **Si+DPA** sample. On the other hand, in the case of **DPA** sample, the maximum J_{SC} is achieved close to the PV cell, with even higher values with respect to SiNCs based LSCs, but these values are fading upon increasing the optical path. For comparison purpose, the J_{SC} value for the DPA sample at 3.5 cm is about 6.5 times and 9 times lower than **Si-DPA** and **Si+DPA** samples, respectively. Once again, this behavior is the typical fingerprint of re-absorption process for a low Stokes-shift, highly luminescent organic luminophore and demonstrated the superior properties of the hybrid organic-inorganic material in real-size devices, where the typical panel size will largely exceed the one employed for this proof-of-concept study.

CONCLUSIONS

We have realized the first example of LSC based on hybrid organic-inorganic silicon nanocrystals able to couple the absorption properties of an organic dye, namely 9-10-diphenylanthracene, with re-absorption free luminescent SiNCs.

The PL and photovoltaic properties were compared for LSCs based on: (i) only the organic chromophore (**DPA**), (ii) only SiNCs (**Si**), a physical mixture of the two components (**Si+DPA**) and a covalent system (**Si-DPA**).

This item was downloaded from IRIS Università di Bologna (<https://cris.unibo.it/>)

When citing, please refer to the published version.

The resulting LSCs are transparent and practical achromatic since DPA absorbs only in the UV region and the SiNC concentration was kept quite low. In the cases of **Si**, **Si+DPA** and **Si-DPA**, losses due to reabsorption of the DPA luminescence by DPA chromophores is minimized, so that a much larger fraction of emitted light is guided to the edges: 74% for **Si**, ca. 55% for **Si-DPA** and **Si+DPA** compared to 31% for **DPA**. SiNC luminescence is not affected by re-absorption phenomena: the shape and intensity of their luminescence bands collected at the edges of LSC devices is practically the same as a function of the distance between excitation and emission, compared to a strong red-shift and decrease in intensity in the case of DPA luminescence. These parameters are very significant in view of the construction of much larger LSC devices where re-absorption losses strongly decrease LSC performances.

The best performances are obtained for **Si+DPA** sample, demonstrating that coupling organic dyes and inorganic silicon nanocrystals is a promising route to enhance LSC performance. Furthermore, its optical and photovoltaic performances are superior also with respect to the covalent system **Si-DPA** because of the decreased PLQY of the Si core upon covalent functionalization. In the **Si+DPA** LSC a trivial energy transfer mechanism, enhanced by the long optical path typically encountered in LSC devices, minimizes the loss due to self re-absorption of DPA luminescence. Optical efficiency as high as 4.25% is achieved with this device architecture without affecting the optimal aesthetic properties of the device, whose high CRI values allow for the utilization of this class of LSCs as solar windows for indoor illumination. This proof of concept opens the way to a new class of hybrid luminophores for LSCs delivering tailored optical properties and high efficiency.

Supporting Information

This item was downloaded from IRIS Università di Bologna (<https://cris.unibo.it/>)

When citing, please refer to the published version.

Supporting Information – Detailed experimental section containing synthetic procedure, LSCs preparation and additional characterization (¹H-NMR, UV-Vis and photovoltaic) is included in the Supporting Information file.

Acknowledgements

R.M. and A.V. acknowledge the Knut & Alice Wallenberg Foundation and the Kempe Foundation for the financial support. A.V. acknowledges the European Union's Horizon 2020 research and innovation programme under grant agreement No 654002 for partial financial support. P.C. acknowledges the University of Bologna for financial support.

Bibliography

- (1) Batchelder, J. S.; Zewail, a H.; Cole, T. Luminescent Solar Concentrators. 1: Theory of Operation and Techniques for Performance Evaluation. *Appl. Opt.* **1979**, *18*, 3090–3110. <https://doi.org/10.1364/AO.18.003090>.
- (2) Debijs, M. G.; Verbunt, P. P. C. Thirty Years of Luminescent Solar Concentrator Research: Solar Energy for the Built Environment. *Adv. Energy Mater.* **2012**, *2*, 12–35. <https://doi.org/10.1002/aenm.201100554>.
- (3) Liu, G.; Mazzaro, R.; Wang, Y.; Zhao, H.; Vomiero, A. High Efficiency Sandwich Structure Luminescent Solar Concentrators Based on Colloidal Quantum Dots. *Nano Energy* **2019**, *60*, 119–126. <https://doi.org/10.1016/j.nanoen.2019.03.038>.
- (4) Jelle, B. P.; Breivik, C.; Drolsum Røkenes, H. Building Integrated Photovoltaic Products: A State-of-the-Art Review and Future Research Opportunities. *Sol. Energy Mater. Sol. Cells* **2012**, *100*, 69–96. <https://doi.org/10.1016/j.solmat.2011.12.016>.
- (5) Meinardi, F.; Bruni, F.; Brovelli, S. Luminescent Solar Concentrators for Building-Integrated Photovoltaics. *Nat. Rev. Mater.* **2017**, *2*, 1–9. <https://doi.org/10.1038/natrevmats.2017.72>.
- (6) Slooff, L. H.; Bende, E. E.; Burgers, A. R.; Budel, T.; Pravettoni, M.; Kenny, R. P.; Dunlop, E. D.; Büchtemann, A. A Luminescent Solar Concentrator with 7.1% Power Conversion Efficiency. *Phys. status solidi - Rapid Res. Lett.* **2008**, *2*, 257–259. <https://doi.org/10.1002/pssr.200802186>.
- (7) Yang, C.; Lunt, R. R. Limits of Visibly Transparent Luminescent Solar Concentrators. *Adv. Opt. Mater.* **2017**, *5*, 1–10. <https://doi.org/10.1002/adom.201600851>.
- (8) Zhao, Y.; Lunt, R. R. Transparent Luminescent Solar Concentrators for Large-Area Solar Windows Enabled by Massive Stokes-Shift Nanocluster Phosphors. *Adv. Energy Mater.* **2013**, *3*, 1143–1148. <https://doi.org/10.1002/aenm.201300173>.
- (9) Correia, S. F. H.; de Zea Bermudez, V.; Ribeiro, S. J. L.; André, P. S.; Ferreira, R. A. S.;

This item was downloaded from IRIS Università di Bologna (<https://cris.unibo.it/>)

When citing, please refer to the published version.

- Carlos, L. D. Luminescent Solar Concentrators: Challenges for Lanthanide-Based Organic–Inorganic Hybrid Materials. *J. Mater. Chem. A* **2014**, *2*, 5580–5596. <https://doi.org/10.1039/C3TA14964A>.
- (10) Gutierrez, G. D.; Coropceanu, I.; Bawendi, M. G.; Swager, T. M. A Low Reabsorbing Luminescent Solar Concentrator Employing π -Conjugated Polymers. *Adv. Mater.* **2016**, *28*, 497–501. <https://doi.org/10.1002/adma.201504358>.
 - (11) Lee, S. M.; Dhar, P.; Chen, H.; Montenegro, A.; Liaw, L.; Kang, D.; Gai, B.; Benderskii, A. V.; Yoon, J. Synergistically Enhanced Performance of Ultrathin Nanostructured Silicon Solar Cells Embedded in Plasmonically Assisted, Multispectral Luminescent Waveguides. *ACS Nano* **2017**, *11*, 4077–4085. <https://doi.org/10.1021/acsnano.7b00777>.
 - (12) Mazzaro, R.; Vomiero, A. The Renaissance of Luminescent Solar Concentrators: The Role of Inorganic Nanomaterials. *Adv. Energy Mater.* **2018**, *8*, 1801903. <https://doi.org/10.1002/aenm.201801903>.
 - (13) Bronstein, N. D.; Yao, Y.; Xu, L.; O'Brien, E.; Powers, A. S.; Ferry, V. E.; Alivisatos, A. P.; Nuzzo, R. G. Quantum Dot Luminescent Concentrator Cavity Exhibiting 30-Fold Concentration. *ACS Photonics* **2015**, *2*, 1576–1583. <https://doi.org/10.1021/acsp Photonics.5b00334>.
 - (14) Li, H.; Wu, K.; Lim, J.; Song, H.-J.; Klimov, V. I. Doctor-Blade Deposition of Quantum Dots onto Standard Window Glass for Low-Loss Large-Area Luminescent Solar Concentrators. *Nat. Energy* **2016**, *1*, 16157. <https://doi.org/10.1038/nenergy.2016.157>.
 - (15) Meinardi, F.; Colombo, A.; Velizhanin, K. A.; Simonutti, R.; Lorenzon, M.; Beverina, L.; Viswanatha, R.; Klimov, V. I.; Brovelli, S. Large-Area Luminescent Solar Concentrators Based on ‘Stokes-Shift-Engineered’ Nanocrystals in a Mass-Polymerized PMMA Matrix. *Nat. Photonics* **2014**, *8*, 392–399. <https://doi.org/10.1038/nphoton.2014.54>.
 - (16) Zhao, H.; Benetti, D.; Jin, L.; Zhou, Y.; Rosei, F.; Vomiero, A. Absorption Enhancement in “Giant” Core/Alloyed-Shell Quantum Dots for Luminescent Solar Concentrator. *Small* **2016**, *12*, 5354–5365. <https://doi.org/10.1002/sml.201600945>.
 - (17) Zhou, Y.; Benetti, D.; Fan, Z.; Zhao, H.; Ma, D.; Govorov, A. O.; Vomiero, A.; Rosei, F. Near Infrared, Highly Efficient Luminescent Solar Concentrators. *Adv. Energy Mater.* **2016**, *6*, 1501913. <https://doi.org/10.1002/aenm.201501913>.
 - (18) Shcherbatyuk, G. V.; Inman, R. H.; Wang, C.; Winston, R.; Ghosh, S. Viability of Using near Infrared PbS Quantum Dots as Active Materials in Luminescent Solar Concentrators. *Appl. Phys. Lett.* **2010**, *96*, 1–4. <https://doi.org/10.1063/1.3422485>.
 - (19) Wei, M.; de Arquer, F. P. G.; Walters, G.; Yang, Z.; Quan, L. N.; Kim, Y.; Sabatini, R.; Quintero-Bermudez, R.; Gao, L.; Fan, J. Z.; et al. Ultrafast Narrowband Exciton Routing within Layered Perovskite Nanoplatelets Enables Low-Loss Luminescent Solar Concentrators. *Nat. Energy* **2019**, No. <https://doi.org/10.1038/s41560-018-0313-y>.
 - (20) Meinardi, F.; Akkerman, Q. A.; Bruni, F.; Park, S.; Mauri, M.; Dang, Z.; Manna, L.; Brovelli, S. Doped Halide Perovskite Nanocrystals for Reabsorption-Free Luminescent Solar Concentrators. *ACS Energy Lett.* **2017**, *2*, 2368–2377. <https://doi.org/10.1021/acsenenergylett.7b00701>.
 - (21) Zhao, H.; Zhou, Y.; Benetti, D.; Ma, D.; Rosei, F. Perovskite Quantum Dots Integrated in Large-Area Luminescent Solar Concentrators. *Nano Energy* **2017**, *37*, 214–223. <https://doi.org/10.1016/j.nanoen.2017.05.030>.
 - (22) Erickson, C. S.; Bradshaw, L. R.; McDowall, S.; Gilbertson, J. D.; Gamelin, D. R.; Patrick,

- D. L. Zero-Reabsorption Doped-Nanocrystal Luminescent Solar Concentrators. *ACS Nano* **2014**, *8*, 3461–3467. <https://doi.org/10.1021/nn406360w>.
- (23) Meinardi, F.; McDaniel, H.; Carulli, F.; Colombo, A.; Velizhanin, K. A.; Makarov, N. S.; Simonutti, R.; Klimov, V. I.; Brovelli, S. Highly Efficient Large-Area Colourless Luminescent Solar Concentrators Using Heavy-Metal-Free Colloidal Quantum Dots. *Nat. Nanotechnol.* **2015**, *10*, 878–885. <https://doi.org/10.1038/nnano.2015.178>.
- (24) Li, Y.; Miao, P.; Zhou, W.; GONG, X.; Zhao, X. N-Doped Carbon-Dots for Luminescent Solar Concentrators. *J. Mater. Chem. A* **2017**, *5*, 21452–21459. <https://doi.org/10.1039/C7TA05220K>.
- (25) Zhou, Y.; Benetti, D.; Tong, X.; Jin, L.; Wang, Z. M.; Ma, D.; Zhao, H.; Rosei, F. Colloidal Carbon Dots Based Highly Stable Luminescent Solar Concentrators. *Nano Energy* **2018**, *44*, 378–387. <https://doi.org/10.1016/j.nanoen.2017.12.017>.
- (26) Mazzaro, R.; Romano, F.; Ceroni, P. Long-Lived Luminescence of Silicon Nanocrystals: From Principles to Applications. *Phys. Chem. Chem. Phys.* **2017**, *19*, 26507–26526. <https://doi.org/10.1039/C7CP05208A>.
- (27) Yu, Y.; Fan, G.; Fermi, A.; Mazzaro, R.; Morandi, V.; Ceroni, P.; Smilgies, D.-M. ; Korgel, B. A. Size-Dependent Photoluminescence Efficiency of Silicon Nanocrystal Quantum Dots. *J. Phys. Chem. C* **2017**, *121*, 23240–23248. <https://doi.org/10.1021/acs.jpcc.7b08054>.
- (28) Meinardi, F.; Ehrenberg, S.; Dharmo, L.; Carulli, F.; Mauri, M.; Bruni, F.; Simonutti, R.; Kortshagen, U.; Brovelli, S. Highly Efficient Luminescent Solar Concentrators Based on Earth-Abundant Indirect-Bandgap Silicon Quantum Dots. *Nat. Photonics* **2017**, *11*, 177–185. <https://doi.org/10.1038/nphoton.2017.5>.
- (29) Wu, K.; Li, H.; Klimov, V. I. Tandem Luminescent Solar Concentrators Based on Engineered Quantum Dots. *Nat. Photonics* **2018**, *12*, 105–110. <https://doi.org/10.1038/s41566-017-0070-7>.
- (30) Romano, F.; Yu, Y.; Korgel, B. A.; Bergamini, G.; Ceroni, P. Light-Harvesting Antennae Based on Silicon Nanocrystals. *Top. Curr. Chem.* **2016**, *374*. <https://doi.org/10.1007/s41061-016-0056-9>.
- (31) Locritani, M.; Yu, Y.; Bergamini, G.; Baroncini, M.; Molloy, J. K.; Korgel, B. A.; Ceroni, P. Silicon Nanocrystals Functionalized with Pyrene Units: Efficient Light-Harvesting Antennae with Bright Near-Infrared Emission. *J. Phys. Chem. Lett.* **2014**, *5*, 3325–3329. <https://doi.org/10.1021/jz501609e>.
- (32) Mazzaro, R.; Locritani, M.; Molloy, J. K.; Montalti, M.; Yu, Y.; Korgel, B. a.; Bergamini, G.; Morandi, V.; Ceroni, P. Photoinduced Processes between Pyrene-Functionalized Silicon Nanocrystals and Carbon Allotropes. *Chem. Mater.* **2015**, *27*, 4390–4397. <https://doi.org/10.1021/acs.chemmater.5b01769>.
- (33) Fermi, A.; Locritani, M.; Di Carlo, G.; Pizzotti, M.; Caramori, S.; Yu, Y.; Korgel, B. A.; Bergamini, G.; Ceroni, P. Light-Harvesting Antennae Based on Photoactive Silicon Nanocrystals Functionalized with Porphyrin Chromophores. *Faraday Discuss.* **2015**, *185*, 481–495. <https://doi.org/10.1039/C5FD00098J>.
- (34) Ravotto, L.; Chen, Q.; Ma, Y.; Vinogradov, S. A.; Locritani, M.; Bergamini, G.; Negri, F.; Yu, Y.; Korgel, B. A.; Ceroni, P. Bright Long-Lived Luminescence of Silicon Nanocrystals Sensitized by Two-Photon Absorbing Antenna. *Chem* **2017**, *2*, 550–560. <https://doi.org/10.1016/j.chempr.2017.02.007>.
- (35) Hessel, C. M.; Reid, D.; Panthani, M. G.; Rasch, M. R.; Goodfellow, B. W.; Wei, J.; Fujii,

- H.; Akhavan, V.; Korgel, B. a. Synthesis of Ligand-Stabilized Silicon Nanocrystals with Size-Dependent Photoluminescence Spanning Visible to Near-Infrared Wavelengths. *Chem. Mater.* **2012**, *24*, 393–401. <https://doi.org/10.1021/cm2032866>.
- (36) Hessel, C. M.; Henderson, E. J.; Veinot, J. G. C. Hydrogen Silsesquioxane: A Molecular Precursor for Nanocrystalline Si-SiO₂ Composites and Freestanding Hydride-Surface-Terminated Silicon Nanoparticles. *Chem. Mater.* **2006**, *18*, 6139–6146. <https://doi.org/10.1021/cm0602803>.
- (37) Arrigo, A.; Mazzaro, R.; Romano, F.; Bergamini, G.; Ceroni, P. Photoinduced Electron-Transfer Quenching of Luminescent Silicon Nanocrystals as a Way To Estimate the Position of the Conduction and Valence Bands by Marcus Theory. *Chem. Mater.* **2016**, *28*, 6664–6671. <https://doi.org/10.1021/acs.chemmater.6b02880>.
- (38) Veinot, J. G. C. et al. Photoluminescent Silicon Nanocrystals with Chlorosilane Surfaces – Synthesis and Reactivity. *Nanoscale* **2015**, *7*, 914–918.
- (39) Montalti, M.; Credi, A.; Prodi, L.; Gandolfi, M. T. *Handbook of Photochemistry*, Third.; CRC Press, 2006.
- (40) Coropceanu, I.; Bawendi, M. G. Core/Shell Quantum Dot Based Luminescent Solar Concentrators with Reduced Reabsorption and Enhanced Efficiency. *Nano Lett.* **2014**, *14*, 4097–4101. <https://doi.org/10.1021/nl501627e>.
- (41) Klimov, V. I.; Baker, T. A.; Lim, J.; Velizhanin, K. A.; McDaniel, H. Quality Factor of Luminescent Solar Concentrators and Practical Concentration Limits Attainable with Semiconductor Quantum Dots. *ACS Photonics* **2016**, *3*, 1138–1148. <https://doi.org/10.1021/acsp Photonics.6b00307>.
- (42) Zhou, Y.; Benetti, D.; Fan, Z.; Zhao, H.; Ma, D.; Govorov, A. O.; Vomiero, A.; Rosei, F. Near Infrared, Highly Efficient Luminescent Solar Concentrators. *Adv. Energy Mater.* **2016**, *6*, 1501913. <https://doi.org/10.1002/aenm.201501913>.

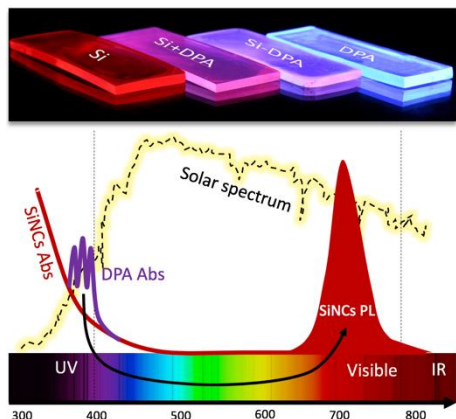
Table of contents

Luminescent Solar concentrators (LSCs) based on Silicon Nanocrystals coupled with 9-10 Diphenylanthracene, with enhanced performance in the UV region of the solar spectrum and transparent, colorless aesthetics for Building Integrated Photovoltaics.

ToC keyword Luminescent Solar Concentrators

Raffaello Mazzaro, Alessandro Gradone, Sara Angeloni, Giacomo Morselli, Pier Giorgio Cozzi, Francesco Romano*, Alberto Vomiero, Paola Ceroni**

Hybrid Silicon nanocrystals for reabsorption-free and transparent luminescent solar concentrators



This item was downloaded from IRIS Università di Bologna (<https://cris.unibo.it/>)

When citing, please refer to the published version.